Fano resonances in plasmonic nanoarrays

Author: Joan Núñez Corbacho
Facultat de Física, Universitat de Barcelona, Diagonal 645, 08028 Barcelona, Spain.

Advisor: Amílcar Labarta Rodríguez - Javier Rodríguez Álvarez

Abstract: We studied some examples of Fano resonances in Plasmonics. In particular, we discuss the hybridization between the broad spectrum of localized surface plasmon resonances and the energy-discrete opening of a diffraction channel in a square lattice of Au nanobars. Our results evidence the broad phenomenology regarding Fano resonances, ranging from a substantial magnification of the system response to a hindering of the excitation.

I. INTRODUCTION

One of the few phenomena ubiquitous in Physics are resonances, where an increase in a certain physical magnitude is caused by the interaction of two periodical systems. One of the most common kinds of resonances have a symmetrical response regarding their spectral shapes that can be modeled by the so called Lorentzian curve:

$$L(E) = \frac{1}{1 + \left(\frac{E - E_p}{\Gamma_p/2}\right)^2}, \tag{1}$$

where E is the energy of the resonance, E_p is the value of the energy corresponding to the maximum amplitude of the resonance, and Γ_p is its spectral width. In the last century a different kind of phenomenon was discovered: Fano resonances.[1] This kind of excitation generally arises under the hybridization of a broad and a sharp-spectrum excitations. For instance, the autoionization of an atom via Auger emission, where an electron of an excited atom transitions to an inner shell and the energy released by this process causes the ejection of a second electron from the atom. This phenomenon can be understood as a hybridization between the energy-discrete transition of the first electron and the continuous energy process of ionization due to the emission of the second electron. The resulting absorption spectra of the system shows a highly asymmetric character that is distinctive of Fano resonances and is modeled by the line-shape

$$F(\xi) = \frac{(\xi + q)^2}{1 + \xi^2}, \tag{2}$$

for $\xi = (E - E_f)/\Gamma$ being the reduced energy, where E_f an Γ are, respectively, the energy at the maximum of the sharp resonance and the width of the corresponding peak, and q is the so called asymmetry parameter. In this work, we aim at studying Fano resonances in Plasmonics. This field carries out the study of surface plasmons, the coupling between the surface conduction electrons in metals and electromagnetic waves. Our matter of study will be Localized Surface Plasmons (LSP), a non-propagating excitation which is observable when an electromagnetic wave with wavelength λ interacts with a metal nanostructure smaller than λ. In this scenario, the electric field of the wave interacts with the electrons at the metal surface inducing localized charge oscillations that, in turn, are coupled to the original electromagnetic field, giving rise to a symmetrical resonance. This originates an electric field in the vicinity of the metal, an example of which can be found in Fig.1(a). When incident radiation is suppressed, the charge oscillation dampens as its energy is absorbed by the bulk of the metal and radiated out by the accelerated charges. This process follows a Lorentzian line-shape and its characteristic lifetime is inversely proportional to the width of the resonance peak, normally in the order of 100 nm, as shown by the extinction cross-section σ_e of an Au nanobar in Fig.1(c).[2]

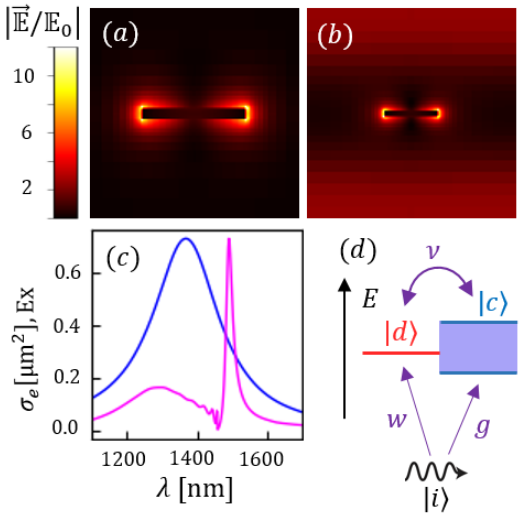

FIG. 1: Panels (a) and (b) show the enhancement of the electric field $|\vec{\mathbb{E}}/\mathbb{E}_0|$ surrounding a isolated Au nanobar for a LSP, and for a SLR in a square array of the same nanoelements, respectively. Panel (c) shows the extinction cross-section σ_e for a single bar (blue curve) and the extinction Ex for the square array (magenta curve). These quantities are properly defined in section II. Panel (d) shows a schematic of the coupling parameters among a photon, a discrete state, and a continuous energy state.

However, these peaks can be narrowed by arranging the metallic elements in an array, so that the far-field radiation emitted from one element interacts with an-

other, preventing the dampening effect. Moreover, under certain conditions, the scattered radiation from different array elements can build a constructive interference, magnifying the LSP significantly via diffraction. This excitations are called Surface Lattice Resonances, or SLR. An example of this is given in Fig.1(b), where high values of the electric field far away from the metal can be observed, due to the constructive interference among the light scattered by the elements of the array. Furthermore, as it is shown in Fig.1(c), SLR show much sharper spectral peaks, in the order of 10 nm, which implies that their life-times are longer.[3]

As this last phenomenon consists on a hybridization between the LSP and the energy-sharp creation of the diffraction channel, we should expect a Fano-like lineshape, as shown by the Ex in Fig.1(c). In fact, we show in section II that the SLR can be modeled by Eq.2, where ξ and q will also be a function of the coupling parameters: ν, between LSP and SLR; w, between the electromagnetic wave and the diffraction channel; and g, between the electromagnetic wave and the LSP.[4] These parameters are schematized in Fig.1(d).

The aim of our work will be to study the SLR excitation taking profit of the easy to manipulate nature of the diffraction through the system geometry, which will allow us to create diverse tailor-made Fano resonances and effectively characterize this phenomenon.

II. SYSTEM AND SIMULATION SETUP

In this work, we present the results of different simulations of plasmonic excitations performed with Lumerical's Finite-Difference Time-Domain (FDTD) software[5], which is capable of solving Maxwell's equations in the Time Domain via the finite difference numerical approximation. More information is given on Appendix V B.

The system consisted in Au bars of length l and square base of edge $d < l$, placed on a square Bravais lattice with periodicity Λ, formally known as pitch, and arranged as shown in Fig.2(a). Then, a short quasi-monochromatic pulse was shot perpendicularly to the array, with its electric field parallel to the long axis of the bars. With this setup, the electric field distribution and the following two quantities were computed: the fraction of the incoming radiation scattered back to the source, known as reflectance (R); and the fraction of the incoming radiation that passed through the array without interacting, known as transmittance (T). Other relevant magnitudes include the absorbance (A), corresponding to the fraction of the incident energy absorbed by the system, calculated as $A = 1 - R - T$, and the extinction (Ex), the fraction of the incident radiation that interacts with the system, which can be calculated as $Ex = 1 - T$.

The latter will be our figure of merit, as it is related to the extinction cross-section σ_e, which is the probability that radiation interacts with a single metallic nanostructure through a plasmonic resonance. Other relevant magnitudes for the LSP are the absorption cross-section σ_a and the scattering cross-section σ_s, the probabilities that radiation is absorbed and scattered through a plasmonic resonance of a single element, respectively.

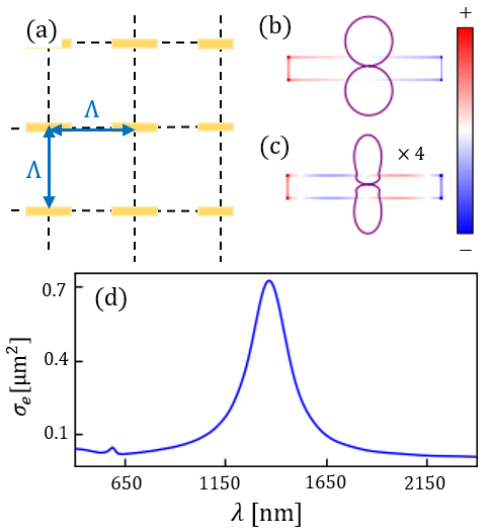

FIG. 2: Geometrical arrangement of the system (a). Charge and angular scattering distributions for the dipole (b) and tetrapole (c) modes of a single bar. The angular scattering in (c) has been scaled up for the sake of clarity. Panel (d) shows σ_e of a single bar as a function of λ.

Taking control of parameters such as the range of λ or the size of the bars allowed us to study the SLR resulting in the hybridization of the diffraction channel with basically two different kinds of LSP. The first one showed a localization of opposite charge at both ends of the bar, as shown in Fig.2(b). The angular scattering distribution of this LSP is also shown in Fig.2(b), being like that of a dipole. We will refer to this excitation as a dipole mode.

The second excitation, the tetrapole mode, is characterized by a four pole charge distribution, with opposite charge at both ends of the bar and between the center and each end of the bar, as can be seen in Fig.2(c). In this case, the angular scattering profile (see Fig.2(c)) exhibits a considerably lower magnitude than the dipole one, which will be significant for the discussion in section III.

In Fig. 2(d), the extinction cross-section σ_e of an Au bar is shown. Two peaks can be recognized, the bigger one corresponding to the dipole mode and the smaller one, at lower wavelengths, corresponding to the tetrapole mode. All results will be discussed under the Fano model, in which σ_e of a single bar can be modified into the extinction Ex of the plasmonic array via the equation

$$Ex(E) = \frac{(\xi(E) + q(E))^2}{1 + \xi(E)^2}\sigma_e(E), \tag{3}$$

where now all Fano parameters are dependent on the energy E and the coupling parameters ν, w, and g, under

the relations[6]

$$q(E) = \frac{\nu w/g}{\Gamma_m(E)/2} + \frac{E - E_p}{\Gamma_p/2}, \tag{4a}$$

$$\xi(E) = \frac{E - E_d}{\Gamma_m(E)/2} - \frac{E - E_p}{\Gamma_p/2} \tag{4b}$$

with $\Gamma_m(E) = 2\pi\nu^2\mathcal{L}(E)$, a new parameter related to the SLR spectral width, where $\mathcal{L}(E)$ is the Lorentzian distribution function $\mathcal{L}(E) = L(E)/\pi\Gamma_p$, for $L(E)$ defined in Eq.1. More details are given on Appendix V A. It should be noted that the coupling parameters will depend on various factors that will characterize how good the two excitations hybridize.

III. RESULTS AND DISCUSSION

Here we present the results of our simulations for the two cases studied. Both of them confirm that SLR exhibit one of the assymetries characterizing Fano resonances: the response of the system varies depending on the relationship between the energies of the two excitations forming the hybridization. This translates into the fact that the behavior of SLR will not be the same whether the diffraction channel has lower or higher energy than the base LSP. Given that all these excitations are driven by electromagnetic radiation, it is more convenient to study this assymetry in geometrical terms and take into account the relation between the wavelengths of the LSP and the diffraction channel. For the former, this will be λ_p, the wavelength at which the extinction of the LSP excitation is maximum; and for the latter, the wavelength of the excitation will be the pitch of the array, Λ.

A. Dipole mode hybridization

In this part of our work, we excited the dipole mode of an Au bar of $l = 400$ nm and $d = 40$ nm. The array pitches were between $\Lambda = 800$ nm and $\Lambda = 1600$ nm and λ of the incident radiation was within $1100 - 1700$ nm.

Our results show that SLR manifest the energy assymetry we introduced earlier. In Fig.3, we show how the electric field intensity varies in one Bravais cell, along the direction perpendicular to the long axis of the bar passing through its center, measured at the λ for which the Ex of each system is maximum, λ_m. Taking into account that the maximum of the dipole mode corresponds to $\lambda_p = 1375$ nm, it is clear that the electromagnetic response behaves differently depending on whether Λ is greater or less than λ_p. In fact, when $\Lambda < \lambda_p$, the electric field is concentrated near the bar, exhibiting a similar response to that of a LSP. However, as Λ increases, the electric field grows far away from the bar. For very high pitches, when $\Lambda > \lambda_p$, the electric field develops a maximum at the border of the Bravais cell, just at the midpoint between the nearest neighbors of the array. This

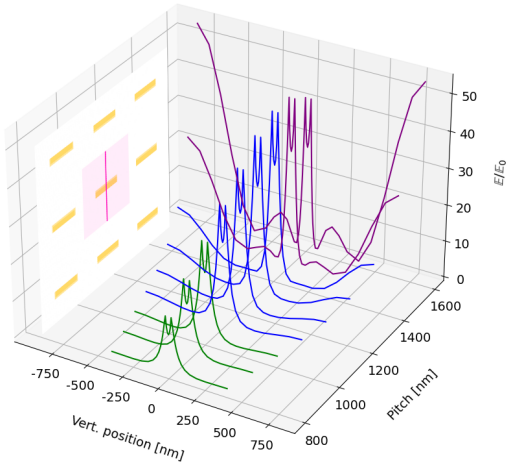

FIG. 3: Electric field enhancement profiles on a Bravais cell along the direction indicated in the inset, computed 10 nm over the bars for the dipole mode, at $\lambda = \lambda_m$ for each case. Three colors were added to better distinguish the three different behavior regimes, being green for low pitches, blue for intermediate pitches, and purple for high pitches.

field distribution is a direct effect of the constructive interference among the scattered radiation by the elements of the lattice, meaning, of the diffraction.

Furthermore, the electric field enhancement reaches much higher values when the diffraction dominates over the LSP, due to the fact that the scattered energy of a single element still interacts with the system and it is not radiated away. Moreover, it can be observed that, for Λ on the order of λ_p, an intermediate region exists where the system is not entirely dominated by the LSP nor the diffraction. In fact, for these values of Λ, the principal contribution to the electric field is still near the bar, but the array effects start to be noticeable in the form of curvature in the field profile far away from the bar. Also, in this region, the field enhancement over the array exhibits a maximum and then starts decreasing as Λ reduces. This effect can be understood in terms of the depolaraizing effect that starts to take place as dipoles get closer to each other. So, more energy is required to sustain the dipole charge distribution and less is radiated into the near field.

One of the factors determining the intensity of this enhancement is the quality of the diffraction process. Under perpendicular incidence, the bars will scatter radiation as shown in Fig.4(a). In particular, for $\lambda = \Lambda$, the diffracted beams are in-plane. Then, the intensity of the scattered wave can be roughly estimated by the scattering efficiency $\varepsilon_s = \sigma_s/S$, where S is the geometrical area of the scatterer perpendicular to the incident wave. So, at the maximum of the LSP, $\varepsilon_s \approx 35 \gg 1$, indicating that the magnitude of the diffraction will be considerable and high hybridization between the two excitations is expected.

A further indicator of this good mixing lies in the Ex spectrum. For all the studied cases, two peaks could be

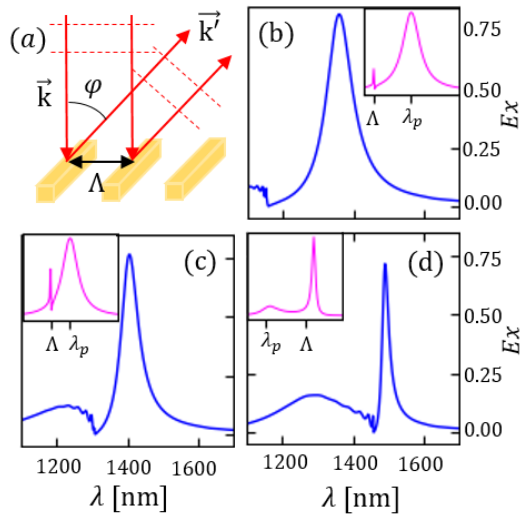

FIG. 4: Diagram of the diffraction ocurring in the array (a). Panels (b), (c), and (d) show Ex as a function of λ for Λ equal to 1150 nm (b), 1300 nm (c), and 1450 nm (d). Plots of the Fano model calculated using Eq.3 are included in the insets, with parameters ν and w/g equal to 2.5, 0 (b) and (c), and 12 and 6 (d). The units of ν are in terms of the discrete excitation width.

identified by looking at whether the electric field was concentrated over the bars or at the space between them. It was found that one of the peaks corresponded to a LSP-dominated excitation and the other one to a diffraction-dominated excitation. Three illustrative examples can be found in Fig.4. These spectra can be seen as the perturbation of the single bar σ_e, shown in Fig.2(d). Interestingly, for low and medium Λ, the dominant peak resembles the symmetric peak of the isolated bar, but, for higher Λ, the dominant peak bears an asymmetric line-shape, corresponding to the hybridization with the diffraction. Also, for $\Lambda < \lambda_p$, the dominant peak appears at λ similar to λ_p and the other one near Λ, but for $\Lambda > \lambda_p$, the bigger one appears near Λ and the smaller one appears left of λ_p. In other words, the excitation with lower energy is magnified by the hybridization and the other one is reduced and pushed to higher energies.

Finally, another way to interpret these results is by using Eq.3-4a-4b, and the parameters corresponding to σ_e of the LSP excitations. Playing with the free coupling parameters ν and w/g, we can approximate a line-shape bearing the relevant characteristics of $Ex(E)$ that will be informative of the nature of the hybridization. For our case, when the LSP dominates over the diffraction, our data resembles a line-shape with $w/g \approx 0$, indicating that the direct coupling of the photons with the diffraction channel is very weak and the excitation of this mode takes place essentially through the LSP. The opposite case happens for high Λ, when the array-effect dominates and $w/g > 1$. In every case, the mixing factor ν is high, indicating that the coupling between the two excitations is strong and the hybridization is favored.[6]

B. Tetrapole mode hybridization

The second kind of simulations performed studied the tetrapole mode with an Au bar with $l = 800$ nm and $d = 20$ nm, with λ between 1000 and 1400 nm. Now $\lambda_p = 1170$ nm, so Λ was in between 1000 and 1350 nm.

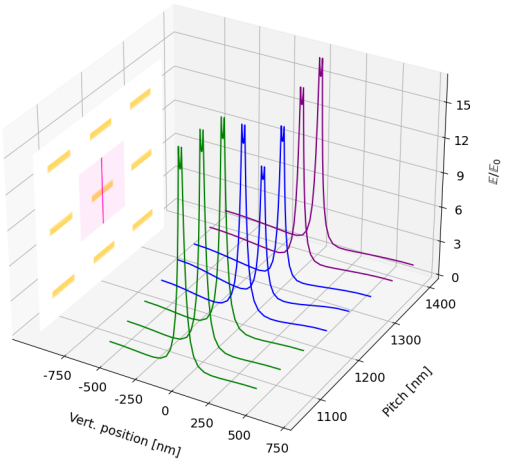

FIG. 5: Electric field enhancement profiles on a Bravais cell along the direction indicated in the inset, computed 10 nm over the bars for the tetrapole mode, at $\lambda = \lambda_m$ for each case. Three colors were added to better distinguish the three different behavior regimes, being green for low pitches, blue for intermediate pitches, and purple for high pitches.

Now, simulations show that LSP does not hybridize well with the diffraction channel. In fact, rather than magnifying the response of the system, the array effect seems to hinder the LSP. One indicator of this is again at the electric field profile shown in Fig.5. Now, the field distribution is concentrated near the bars for all Λ, indicating that the LSP always dominates, in contrast with the dipole mode. Nevertheless, array effects can be perceived for $\Lambda \approx \lambda_p$ as the faint curvature in the profile lines near the borders of the Bravais cell, but they are almost negligible. Furthermore, instead of reaching a maximum, the field enhancement reaches a minimum, further indicating that now LSP and diffraction do not hybridize well.

An indicator of this poor hybridization can be found again in the quality of the diffraction process. As shown in Fig.6(a), now the optical response of the LSP is dominated by σ_a, being σ_s considerably lower. Quantitatively, $\varepsilon_s \approx 1$, in contrast with the dipole mode. Then, only a poor hybridization of the two excitations is expected.

In addition, Ex spectra shown in Fig.6(b)-(d) all resemble the Lorentzian profile characterizing LSP, with a dip about $\lambda = \Lambda$. Therefore, the two excitations do not add up, but instead, the array interferes with the LSP tampering its optical response.

By using Eq.3-4a-4b, we can produce similar line-shapes as those obtained in our simulations. Now, all of them comprise low values of both w/g and ν, indicating that the continuous LSP always dominates over

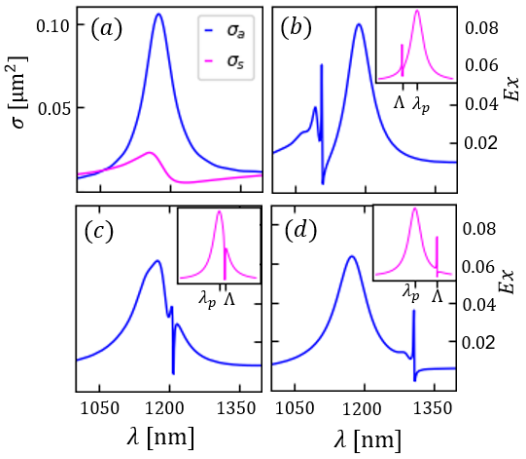

FIG. 6: Absorption cross-section σ_a and scattering cross-section σ_s as a function of λ for the $800\times20\times20$ nm^3 bar (a). Panels (b), (c) and (d) show Ex as a function of λ for Λ equal to 1100 nm (b), 1200 nm (c), and 1300 nm (d). Plots of the Fano model calculated using Eq.3 are included in the insets, with parameters ν and w/g equal to 0.015 and 0.015 (b), and 0.03 and 0.05 (c) and (d). The units of ν are in terms of the discrete excitation width.

the discrete diffraction and that the two excitations hybridize poorly, as expected. These values reflect the weak coupling between the photon and the diffraction channel explaining the low quality of the hybridization. Consequently, the diffraction tampers the LSP instead of magnifying it, unlike the case of the dipole mode.

C. Comparison between both modes

In order to characterize the nature of the hybridization giving rise to the SLR it is useful to look at which λ_m the optical response of the system is maximum. In Fig.7, we plot λ_m as a function of Λ for the two LSP studied. Fig.7(a) shows that for the dipole mode the three regimes described in section III A can be recognized. For lower Λ, λ_m is near λ_p as the LSP dominates and decreases as the bars get closer together because of the depolarizing effect. For higher Λ, instead, the diffraction dominates, and so $\lambda_m \approx \Lambda$. This behavior is characteristic of a crossing interaction between the two resonances.

On the other hand, in Fig. 7(b), the behavior is completely different. For $\Lambda < \lambda_p$, λ_m is near λ_p, meaning that the LSP still dominates with a small influence of the array. However, now, for $\Lambda > \lambda_p$, the diffraction effect becomes completely negligible as $\lambda_m = \lambda_p$. Interestingly, when $\Lambda \approx \lambda_p$, λ_m seems to increase, a sign that the two excitations seem to repel each other. All this phenomenology indicats a kind of anticrossing between the two resonances.

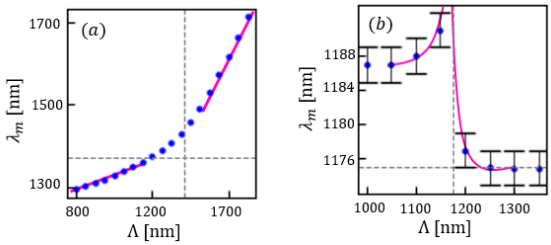

FIG. 7: λ_m as a function of Λ for the dipole mode-SLR (a) and the tetrapole mode-SLR (b). The gray dashed lines correspond to $\Lambda = \lambda_p$ and $\lambda_m = \lambda_p$, and the magenta lines sketch the assymptotical behavior of the data. Error bars for the data in panel (a) are about the size of the dots. Error bars are included for panel (b) with the spectral resolution of our simulations.

IV. CONCLUSIONS

We have shown that SLR can be described as the hybridization between LSP and a diffraction channel, and that the characteristics of each excitation determine the quality of the resonance. We have also shown two different cases of this hybridization, a crossing and an anticrossing. We can conclude that when the coupling of the incident photons with the diffraction is strong, the response of the system is magnified, and SLR can either be determined by LSP or diffraction; but when the coupling is weak, the array effect induces destructive interference between its elements, and SLR only exhibits features of a hindered LSP.

Acknowledgments

There are not enough words in this language to express the magnitude of my gratitude to both of my advisors.

[1] U. Fano, "Effects of configuration interaction on intensities and phase shifts," *Phys. Rev.*, vol. 124, pp. 1866–1878, Dec 1961. 1

[2] S. Maier, *Plasmonics: Fundamentals and Applications*. Springer US, 2007. 1

[3] V. G. Kravets, A. V. Kabashin, W. L. Barnes, and A. N. Grigorenko, "Plasmonic surface lattice resonances: A review of properties and applications," *Chemical Reviews*, vol. 118, no. 12, pp. 5912–5951, 2018. 2

[4] Y. Francescato, V. Giannini, and S. A. Maier, "Plasmonic systems unveiled by fano resonances," *ACS Nano*, vol. 6, no. 2, pp. 1830–1838, 2012. 2

[5] Lumerical Inc. - Innovative Photonic Design Tools. [Online]. Available: https://www.lumerical.com/ (accessed on Feb 20, 2023). 2, 6

[6] V. Giannini, Y. Francescato, H. Amrania, C. C. Phillips, and S. A. Maier, "Fano resonances in nanoscale plasmonic systems: A parameter-free modeling approach," *Nano Letters*, vol. 11, no. 7, pp. 2835–2840, 2011. 3, 4, 6

V. APPENDIX

A. Fano Model in Plasmonics

In this section we aim at showing that SLR are expected to follow a Fano line-shape as described in Eq.2. For that purpose, we shall adopt Dirac's formalism, under which the SLR will be a mixed state $|\Psi\rangle$ between a quasi continuous state $|c\rangle$, corresponding to the LSP, and a discrete state $|d\rangle$, the opening of the diffraction channel. We can introduce the independent Hamiltonian $\mathcal{H}_0$, such that $\langle c'|\,\mathcal{H}_0\,|c\rangle = E_c\delta(c-c')$, $\langle d|\,\mathcal{H}_0\,|d\rangle = E_d$, and $\langle c|\,\mathcal{H}_0\,|d\rangle = 0$. Then, we can induce a mixing of the two states as a perturbation $\mathcal{H}'$ such that $\langle c|\,\mathcal{H}'\,|d\rangle = \nu\sqrt{\mathcal{L}(E)}$, where ν is a real mixing parameter and $\mathcal{L}(E)$ is the Lorentzian distribution function equal to $\mathcal{L}(E) = L(E)/\pi\Gamma_p$, for $L(E)$ defined in Eq.1. In other words, we are considering a system with well-defined energy states and we are introducing a small mixing between them, with the reasonable assumption that the mixing factor is proportional to the line-shape of the continuous state, meaning $|\langle c|\,\mathcal{H}'\,|d\rangle|^2 = \nu^2\mathcal{L}(E)$. Then, the SLR will be the mixed state $|\Psi\rangle$ solution of the eigenvalue equation $\mathcal{H}\,|\Psi\rangle = E\,|\Psi\rangle$, for $\mathcal{H} = \mathcal{H}_0 + \mathcal{H}'$. The interesting part will be that the optical properties of the system can be described by considering the interaction of a photon $|i\rangle$ with the SLR, modeled under a coupling operator W such that $\langle i|\,W\,|d\rangle = w$ and $\langle i|\,W\,|c\rangle = g\sqrt{\mathcal{L}(E)}$, where w and g are the coupling parameters of the photon with the discrete and continuous states, respectively; and the same assumption of proportionality to the line-shape has been made. This way, we should be able to reproduce how the LSP is modified into the SLR via the magnitude[6]

$$F(E) = \frac{|\langle i|\,W\,|\Psi\rangle|^2}{|\langle i|\,W\,|c\rangle|^2}. \tag{5}$$

Surprisingly, this quantity can be calculated as a function of only the mixing parameters ν, w, and g, by computing $|\Psi\rangle$ as a function of $|c\rangle$ and $|d\rangle$, and then simply calculating $\langle i|\,W\,|\Psi\rangle$. After defining new quantities, one can get

$$F(E) = \frac{(\xi(E) + q(E))^2}{1+\xi(E)^2}, \tag{6}$$

where now all Fano parameters are dependent on the energy E under the relations given in Eq.4a-4b.

B. Lumerical software

All simulations throughout this work were performed using Lumerical's FDTD software.[5] This software's method works by creating a spatial and temporal grid

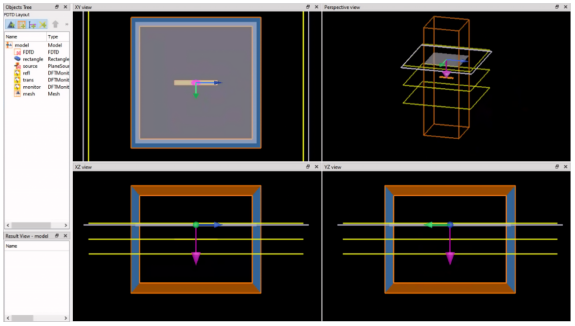

FIG. 8: Screenshot of Lumerical's interface simulating a SLR.

and then solving Maxwell's equations on each point of the grid. Different materials can be defined by giving different values of the refractive index n and the absorption coefficient κ to each point of this mesh. The software included a visual interface, shown in Fig.8, which allows to easily create different simulations by building custom light sources and metallic structures with tabulated values of n and κ. All physical objects needed to be set inside a simulation environment, whose boundaries could be set with periodic boundary conditions, allowing for an effective simulation of an infinite periodic system. The meshing needed to perform the FDTD method can also be customized in order to obtain a good resolution and computing time.